Volume 1 | Number 1 | Jan 2013 | Pages 1–100

Dalton Transactions

An international journal of inorganic chemistry
www.rsc.org/dalton

ROYAL SOCIETY OF CHEMISTRY

ROYAL SOCIETY OF CHEMISTRY

www.rsc.org/dalton

Dalton
Transactions

Dynamic Article Links ▶

COMMUNICATION

Reversible formation of supramolecular polymer networks *via* orthogonal pillar[10]arene-based host–guest interactions and metal ion coordinations

Lintao Wu[1], Chun Han[1], Xi Wu[1], Lei Wang[2], Yaozi Caochen[2], Xiaobi Jing[2]*

Supramolecular polymer networks, assembled *via* the combination of orthogonal terpyridine–Zn^{2+}, carbene–Ag^+, and pillar[10]arene/alkyl chain recognition motifs, exhibit dynamic properties responsive to various external stimuli.

10 In the past few decades, due to their applications in the analytical and biomedical fields, supramolecular polymers, which represent dynamic assembled chains of low molar mass monomers held together by reversible and highly directional noncovalent interactions, and have demonstrated traditional polymeric 15 properties in solution as well as in the bulk, have received considerable attention.[1] On the other hand, pillar[*n*]arenes, are a new class of supramolecular hosts[2] after crown ethers,[3] cyclodextrins,[4] calixarenes,[5] and cucurbiturils.[6] Their synthetic methods,[7] functionalizations,[8] conformations,[9] host–guest 20 properties,[10] self-assembly in water or organic solvents,[11] and applications in different areas such as nanoparticles,[12] drug delivery,[13] and MOFs,[14] have been widely investigated by chemists and materials scientists.[15] Up to now, thanks to the great efforts made by supramolecular chemists, several good examples 25 of supramolecular polymers constructed by pillararene-based molecular recognitions have been reported.[16] However, recent studies about pillararene-based supramolecular polymers mainly focus on pillar[5,6]arenes. Comparatively, little effort has been made to investigate larger size pillar[*n*]arenes,[17] which possess 30 different conformations due to the relatively rigid tetrahedron bonding feature of the methylene bridge, as revealed by the calixarene and cucurbituril series.[18] Especially, larger size pillar[*n*]arenes-based supramolecular polymers have never reported.

35 Herein, we would like to design and synthesize the hierarchical self-assembly of a supramolecular polymer network driven by pillar[10]arene-based host–guest interaction and metallic coordination. Specifically, the terpyridine and imidazolium units are attached on each side of the ligand **1**. Upon addition of metal 40 ions such as Zn^{2+}, it is expected to form dimeric complex **3** through terpyridine–Zn^{2+} coordination. On the other hand, from previous study, we know that one pillar[10]arene can complex with two alkyl chains,[19] so upon addition of pillar[10]arene into the solution of **3** can form the linear supramolecular polymer **A**. 45 Meanwhile, imidazolium units are incorporated into the middle

site of **A**, which are capable of forming an Ag^+ complex after coordination with Ag_2O, thereby inducing the cross-linking of the linear polmers **A**. More interestingly, the supramolecular polymer networks showed dynamic properties responsive to various 50 external stimuli, such as light or addition of competitive guest **5** (Scheme 1).
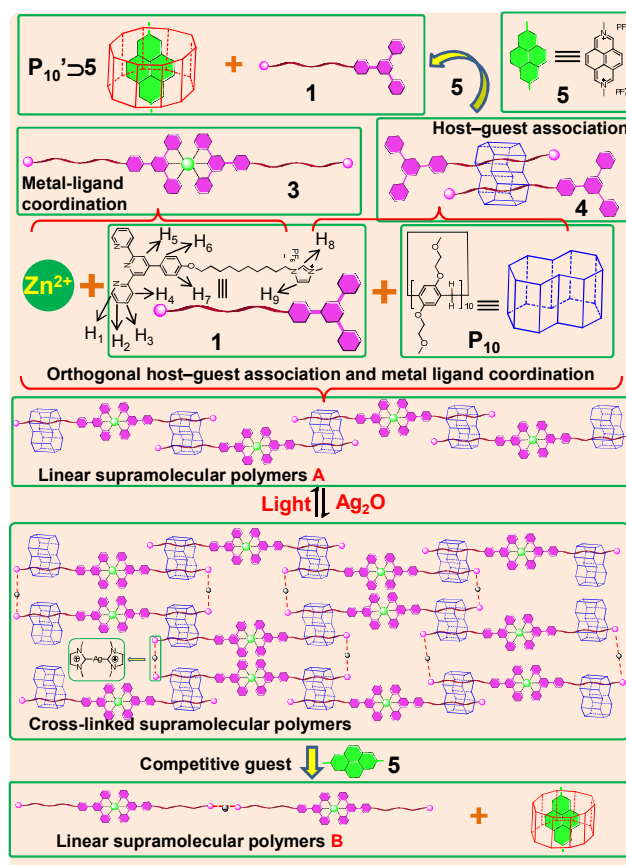
Scheme 1

Scheme 1. Chemical structures of ligand **1**, competitive guest **5**, and pillar[10]arene **P10** and cartoon representations of the formation of supramolecular polymer networks and light or competitive guest **5**-induced morphology transformation.

Ligand **1** was synthesized by three simple steps (Scheme S1, ESI†). The capability to form Zn^{2+}–**1** complex was investigated by UV/Vis measurements. Addition of $Zn(ClO_4)_2$ with ligand **1** shows a clear isosbestic point at 315 nm (Fig. 1a), indicating the efficient conversion from free to metal-complexed terpyridine species. The achievement of maximum absorbance (λ_{max} = 330 nm) at the $Zn(ClO_4)_2$ molar ratio of 0.5 apparently supports the formation of a 2:1 complex for terpyridine and Zn^{2+} (Fig. 1b). ^{1}H NMR also used to show the formation of Zn^{2+}–**1** complex. When the ratio of Zn^{2+}/**1** is 0.5, the terpyridine protons H_2, H_3, and H_4 shifted downfield, while H_1, and H_5 revealed a remarkable upfield, mainly attributing to the shielding effect of the neighboring terpyridine unit (Fig. S5, ESI†). Furthermore, in the electrospray ionization mass spectrum of $Zn(1\text{-}PF_6)_2^{4+}$ (Fig. S6, ESI†), the peaks at m/z = 289.2, which correspond to the fragment of $Zn(1\text{-}PF_6)_2^{4+}$, was observed, confirming the formation of dimeric complex **3**.
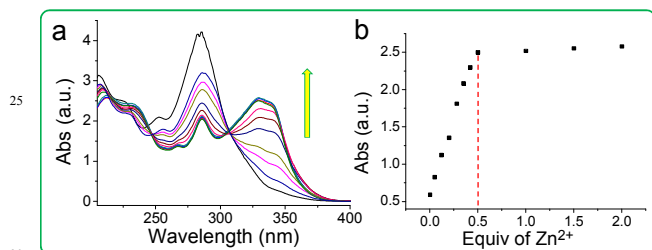

Fig.1 Change in the UV-Vis absorption spectra upon stepwise addition of $Zn(ClO_4)_2$ (1.0 mM in CH_3CN) to a 0.02 mM solution of monomer **1** in CH_3CN. a) UV-Vis absorption spectra. b) The normalized absorbance at 330 nm. The formation of metal–ligand complex was evidenced by a clear isosbestic point at 315 nm, indicating the efficient conversion from free to metal–complexed terpyridine species. The achievement of maximum absorbance (λmax = 330 nm) at the $Zn(ClO_4)_2$/**1** molar ratio of 0.5 apparently supports the formation of $Zn(1\text{-}PF_6)_2^{4+}$ complex.

From previous study by Hou and *co*-workers we know that one pillar[10]arene framework could complex with two alkyl chains.[19] Here, the host–guest complexation between **1** and **P10** was elucidated using the ^{1}H NMR spectrum (Fig. S7, ESI†). Protons H_a, H_b, and H_c on ligand **1** shifted upfield after complexation. Furthermore, the overlapped signal corresponding to H_d was obviously split into several separate peaks (d: 1.21, 1.08, 0.66, 0.31, 0.02, –0.25, –0.78, –0.95, and –1.23 ppm) (Fig. S8, ESI†). On the other hand, no obvious chemical shift change occurs for the terpyridine unit, demonstrating the preferential host–guest complexation without the involvement of the terpyridine ligand. These phenomena suggested that ligand **1** was threaded through the cavity of cyclic host **P10** with its middle methylene groups (H_d) located in the cavity and the terpyridine unit out of the cavity (Scheme 1).

After confirming orthogonal self-assembling properties of ligand **1**–Zn^{2+} and **P10**/alkyl chain recognition motifs, the linear supramolecular polymer **A** was first envisioned to be driven by host–guest interactions and metal coordination in CH_3CN. The concentration-dependent ^{1}H NMR spectra of $\mathbf{1_2 \cdot Zn \cdot P_{10}}$ (400

MHz, CD_3CN, 298 K) provided important insights into their self-assembly behaviors in solution (Fig. 2). As the concentration increased, the signals of protons on the terpyridyl groups became broad at high concentration, indicating that the monomers self-assembled into high-molecular-weight aggregates.
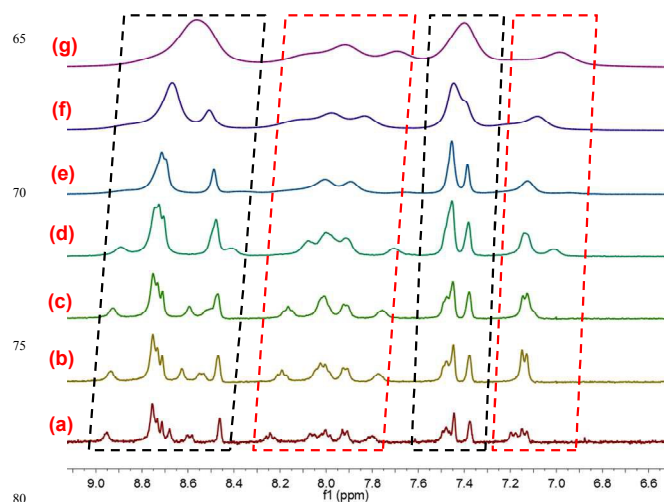

Fig.2 ^{1}H NMR spectra (400 MHz, 298 K, CD_3CN) of $\mathbf{1_2 \cdot Zn \cdot P_{10}}$ (linear supramolecular polymer **A** at various concentrations: (a) 0.50 mM; (b) 5.0 mM; (c) 10.0 mM; (d) 20.0 mM; (e) 40.0 mM; (f) 80.0 mM; and (g) 160 mM.

Further complexation between the imidazolium ligands on linear supramolecular polymer **A** and Ag_2O furnished the desired supramolecular polymer network. After we added excess Ag_2O to a solution of linear supramolecular polymer **A** and stirred it for 12 hours under black, the supramolecular polymer network was successfully prepared. As shown in Fig. S9, the signal of imidazolium proton H_8 disappeared, indicating the formation of carbine-Ag complex.[20] More interestingly, the signal of H_8 reappeared by adding CF_3COOH, which is attributed to the stronger binding ability between Ag^+ and CF_3COOH (Fig. S9). However, when we added NaOH into the solution of linear supramolecular polymer **A**, the signal of H_8 remained the same, suggesting that the complexation was not simply pH-reponsive (Fig. S9, ESI†).

Viscometry is a convenient method to test the propensity of monomers to self-assemble into large aggregates. Therefore, viscosity measurements were carried out in CH_3CN using a Cannon Ubbelohde semi-microdilution viscometer. As presented in Fig. 3 (black lines), the linear supramolecular polymer **A** assembled from the monomers exhibited a viscosity transition that is characterized by a change in slope in the double logarithmic plots of specific viscosity versus concentration. In the low concentration range, the slopes approximated unity, which is characteristic for cyclic oligomers with constant size. When the concentration exceeded the critical polymerization concentration (CPC; approximately 50.0 mM), a sharp rise in the viscosity was observed. The formation of supramolecular polymer networks was also confirmed using viscosity studies (Fig. 3, red lines). The supramolecular polymer networks exhibited higher viscosities than linear polymer **A** at low concentration, which partially results from the polyelectrolyte effect.[21] However, at high concentration, supramolecular polymer networks led to a

decrease in the viscosity. This can be attributed to the influence of metal–ligand interactions on the host–guest aggregation; the linker in linear polymer **A** becomes more rigid after coordination, which is disadvantageous for the entanglement of the supramolecular polymers.
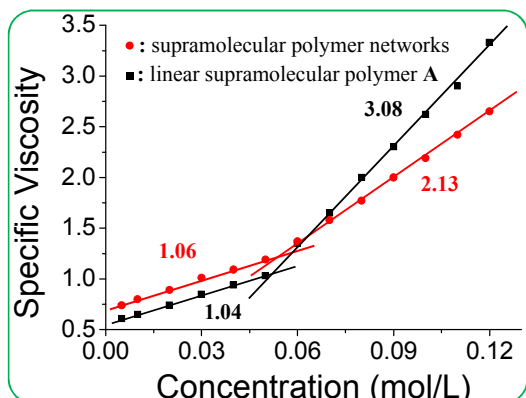
Fig. 3 Specific viscosities of the linear supramolecular polymer **A** and the supramolecular polymer networks in CH$_3$CN at 298 K *versus* monomer concentration.

Furthermore, the morphology of the supramolecular polymer networks was investigated by scanning electron microscopy (SEM) studies. As shown in Fig. 4a, a three-dimensional network was obtained from a highly concentrated solution. Moreover, a rod-like fiber with a regular diameter of 1 μm was drawn from a high concentration solution and observed by SEM (Fig. 4b). All the results above provide efficient evidences for the formation of supramolecular polymer networks with high molecular weight.
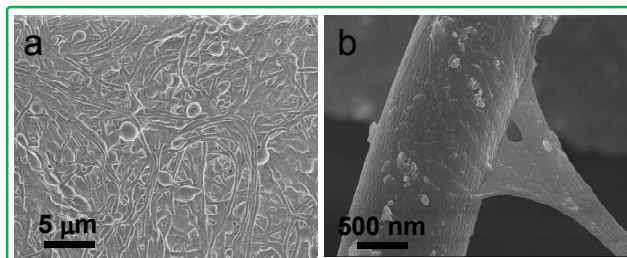
Fig.4 SEM images: (a) the three-dimensional network of the supramolecular polymer network; (b) a rod-like fiber drawn from a high concentration solution of **1$_2$•Zn•P$_{10}$/Ag** in CH$_3$CN.

Lastly, the dynamic macroscopic properties of the high concentration supramolecular polymer networks were also investigated. Glue-like viscous liquids were prepared by dissolving **1$_2$•Zn•P$_{10}$/Ag** at a concentration of 200 mM in CH$_3$CN at 60 °C followed by cooling to room temperature. The high concentration supramolecular polymer networks showed reversible glue–sol phase transitions by heating and cooling (Fig. 5). Furthermore, addition of competitive guest **5** could also induce the glue–sol phase transitions due to the complex constant of **P$_{10}$⊃5** is larger than **P$_{10}$⊃1** (Fig. S10, ESI†). More interestingly, the glue-like supramolecular polymer networks showed light responsive property. As shown in Fig. 5, after exposing the glue-like supramolecular polymer network under visible light for 12h, it transferred into solution. However, it could return to glue-like structure upon addition of Ag$_2$O again

and stirred for 8h in black. Due to CF$_3$COOH bonded with Ag$^+$ firmly, so addition of CF$_3$COOH could also induced Glue-like **1$_2$•Zn•P$_{10}$/Ag** into solution (Fig. 5).
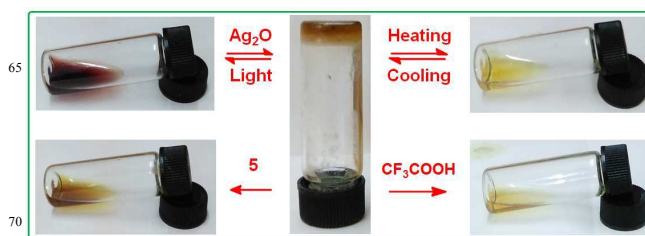

Fig. 5 The glue-sol transitions of the supramolecular polymer networks triggered by different stimuli.

In summary, we have developed a three-step self-assembly pathway to fabricate the supramolecular polymer networks *via* a heterometallic coordination-driven self-assembly strategy. The linear supramolecular polymer **A** was first formed through **P$_{10}$** based host–guest interactions and terpyridine-Zn^{2+} coordination. Subsequently, imidazolium units are incorporated into the middle site of linear supramolecular polymer **A**, allows for the efficient complexation with Ag$_2$O, resulting in the formation of the desired supramolecular polymer networks. Various methods, such as ^{1}H NMR, UV-Vis, SEM, and viscosity measurements were performed to investigate the properties of the resulting supramolecular polymer networks. Moreover, triggered by light, heating addition of competitive ligand **5**, the supramolecular polymer networks could be reversibly assembled/disassembled. Therefore, the current work provides a convenient approach for architecture control of supramolecular polymer networks, which is a prerequisite for future applications of such assemblies as intelligent materials.

Acknowledgements

Notes and references

^{1}*Department of Chemistry, Changzhi University, Changzhi, Shanxi, 046011 (China).*

^{2}*College of Chemistry and Chemical Engineering, Yangzhou University, Yangzhou, Jiangsu, 225002 (China).*

E-mail: xbjing@yzu.edu.cn

† Electronic Supplementary Information (ESI) available: Synthetic procedures, characterizations and other materials. See DOI: 10.1039/b000000x/

1   (*a*) X. Yan, F. Wang, B. Zheng and F. Huang, *Chem. Soc. Rev.*, 2012, **41**, 6042; (*b*) E. A. Appel, J. Barrio, X. J. Loh and O. A. Scherman, *Chem. Soc. Rev.*, 2012, **41**, 6195.
2   T. Ogoshi, S. Kanai, S. Fujinami, T.-A. Yamagishi and Y. Nakamoto, *J. Am. Chem. Soc.*, 2008, **130**, 5022.
3   (*a*) S. J. Loeb and J. A. Wisner, *Angew. Chem., Int. Ed.*, 1998, **37**, 2838; (*b*) Q. Wang, M. Cheng, Y. Zhao, Z. Yang, J. Jiang, L. Wang and Y. Pan, *Chem. Commun.*, 2014, **50**, 15585; (*c*) L. Chen, H.-Y. Zhang, and Y. Liu, *J. Org. Chem.*, 2012, **77**, 9766.

Dalton Transactions Accepted Manuscript

4   A. Harada, Y. Takashima and H. Yamaguchi, *Chem. Soc. Rev.*, 2009, **38**, 875.

5   (*a*) Y. Sun, C.-G. Yan, Y. Yao, Y. Han and M. Shen, *Adv. Funct. Mater.*, 2008, **18**, 3981; (*b*) D. A. Fowler, A. V. Mossine, C. M. Beavers, S. J. Teat, S. J. Dalgarno and J. L. Atwood, *J. Am. Chem. Soc.*, 2011, **133**, 11069; (*c*) D.-S. Guo, K. Wang, Y.-X. Wang and Y. Liu, *J. Am. Chem. Soc.*, 2012, **134**, 10244..

6   (*a*) Y. Jiang, Y. Wang, N. Ma, Z. Wang, M. Smet and X. Zhang, *Langmuir*, 2007, **23**, 4029; (*b*) H. Tang, D. Fuentealba, Y. H. Ko, N. Selvapalam, K. Kim and C. Bohne, *J. Am. Chem. Soc.*, 2011, **133**, 20623; (*c*) F. Biedermann, V. D. Uzunova, O. A. Scherman, W. M. Nau and A. D. Simone, *J. Am. Chem. Soc.*, 2012, **134**, 15318.

7   (*a*) D. Cao, Y. Kou, J. Liang, Z. Chen, L. Wang, and H. Meier, *Angew. Chem. Int. Ed.* 2009, **48**, 9721; (*b*) Y. Ma, Z. Zhang, X. Ji, C. Han, J. He, Z. Abliz, W. Chen, and F. Huang, *Eur. J. Org. Chem.* 2011, 5331; (*c*) T. Ogoshi, N. Ueshima, F. Sakakibara, T.-a. Yamagishi, and T. Haino, *Org. Lett.*, 2014, **16**, 2896.

8   (*a*) L. Chen, Z. Li, Z. Chen, and J.-L. Hou, *Org. Biomol. Chem.*, 2013, **11**, 248; (*b*) C. Han, Z. Zhang, G. Yu, and F. Huang, *Chem. Commun.*, 2012, **48**, 9876.

9   T. Ogoshi, K. Kitajima, T.-a. Yamagishi, and Y. Nakamoto, *Org. Lett.*, 2010, **12**, 636.

10 (*a*) X. Shu, S. Chen, J. Li, Z. Chen, L. Weng, X. Jia, and C. Li, *Chem. Commun.*, 2012, **48**, 2967; (*b*) W. Xia, X.-Y. Hu, Y. Chen, C. Lin, and L. Wang, *Chem. Commun.*, 2013, **49**, 5085; (*c*) C. Li, Q. Xu, J. Li, F. Yao, and X. Jia, *Org. Biomol. Chem.*, 2010, **8**, 1568; (*d*) C. Li, S. Chen, J. Li, K. Han, M. Xu, B. Hu, Y. Yu, and X. Jia, *Chem. Commun.*, 2011, **47**, 11294; (*e*) C. Li, J. Ma, L. Zhao, Y. Zhang, Y. Yu, X. Shu, J. Li, and X. Jia, *Chem. Commun.*, 2013, **49**, 1924; (*f*) W.-B. Hu, W.-J. Hu, X.-L. Zhao, Y. A. Liu, J. –S. Li, B. Jiang, and K. Wen, 2015, **DOI**: 10.1039/c5cc05623c.

11 (*a*) Y. Yao, M. Xue, J. Chen, M. Zhang, and F. Huang, *J. Am. Chem. Soc.*, 2012, **134**, 15712; (*b*) Y. Yao, P. Wei, S. Yue, J. Li, and M. Xue, *RSC Adv.*, 2014, **4**, 6042; (*c*) G. Yu, Y. Ma, C. Han, Y. Yao, G. Tang, Z. Mao, C. Gao, and F. Huang, *J. Am. Chem. Soc.*, 2013, **135**, 10310; (*d*) Z.-Y. Li, Y. Zhang, C.-W. Zhang, L.-J. Chen, C. Wang, H. Tan, Y. Hu, X. Li, and H.-B. Yang, *J. Am. Chem. Soc.*, 2014, **136**, 8577.

12 (*a*) Y. Yao, M. Xue, X. Chi, Y. Ma, J. He, Z. Abliz, and F. Huang, *Chem. Commun.*, 2012, **48**, 6505; (*b*) Y. Yao, X. Chi, Y. Zhou, and F. Huang, *Chem. Sci.*, 2014, **5**, 2778; (*c*) Y. Yao, Y. Wang, and F. Huang, *Chem. Sci.*, 2014, **5**, 4312; (*d*) H. Li, D.-X. Chen, Y.-L. Sun, Y. B. Zheng, L.-L. Tan, P. S. Weiss, and Y.-W. Yang, *J. Am. Chem. Soc.*, 2013, **135**, 1570.

13 Q. Duan, Y. Cao, Y. Li, X. Y. Pan, and L. Wang, *J. Am. Chem. Soc.*, 2013, 135, 10542.

14 N. L. Strutt, D. Fairen-Jimenez, J. Iehl, M. B. Lalonde, R. Q. Snurr, O. K. Farha, J. T. Hupp, and J. F. Stoddart, *J. Am. Chem. Soc.*, 2012, **134**, 17436.

15 (*a*) L. Chen, W. Si, L. Zhang, G. Tang, Z.-T. Li, and J.-L. Hou, *J. Am. Chem. Soc.*, 2013, **135**, 2152; (*b*) J. Zhou, M. Chen, and G. Diao, *Chem. Commun.*, 2014, **50**, 11954; (*c*) Y. Fang, L. Wu, J. Liao, L. Chen, Y. Yang, N. Niu, L. He, S. Zou, W. Feng, and L. Yuan, *RSC Adv.*, 2013, **3**, 12376; (*d*) J. Cao, Y. Shang, B. Qi, X. Sun, L. Zhang, H. Liu, H. Zhang, and X. Zhou, *RSC Adv.*, 2015, **5**, 9993; (*e*) H. Chen, J. Fan, X. Hu, J. Ma, S. Wang, J. Li, Y. Yu, X. Jia, and C. Li, *Chem. Sci.*, 2015, **6**, 197.

16 (*a*) Z. Zhang, Y. Luo, J. Chen, S. Dong, Y. Yu, Z. Ma, and F. Huang, *Angew. Chem. Int. Ed.*, 2011, **50**, 1397; (*b*) X. Wang, K. Han, J. Li, X. Jia, and C. Li, *Polym. Chem.*, 2013, **4**, 3998; (*c*) Y. Guan, M. Ni, X. Hu, T. Xiao, S. Xiong, C. Lin, and L. Wang, *Chem. Commun.*, 2012, **48**, 8529; (*d*) B. Shi, K. Jie, Y. Zhou, D. Yu, and Y. Yao, *Chem. Commun.*, 2015, **51**, 4503; (*e*) Y. Zhou, K. Jie, B. Shi, and Y. Yao, *Chem. Commun.*, 2015, **51**, 11112.

17 Z. Li, J. Yang, G. Yu, J. He, Z. Abliz, and F. Huang, *Chem. Commun.*, 2014, **50**, 2841.

18 J. K. Lee, S. Samal, N. Selvapalam, H.-J. Kim and K. Kim, *Acc. Chem. Res.*, 2003, **36**, 621.

19 X.-B. Hu, Z. Chen, L. Chen, L. Zhang, J.-L. Hou, and Z.-T. Li, *Chem. Commun.*, 2012, **48**, 10999.

20 (*a*) X. Zhang, S. Gu, Q. Xia and W. Chen, *J. Organomet. Chem.*, 2009, **694**, 2359; (*b*) B. Liu, B. Liu, Y. Zhou and W. Chen, *Organometallics*, 2010, **29**, 1457; (*c*) Y. Zhou, Y. Yao, and M. Xue, *Chem. Commun.*, 2014, **50**, 8040.

21 F. Wang, J. Zhang, X. Ding, S. Dong, M. Liu, B. Zheng, S. Li, L. Wu, Y. Yu, H. W. Gibson, and F. Huang, *Angew. Chem. Int. Ed.*, 2010, **49**, 1090.

Colour Graphic:

Text:

Reversible supramolecular polymer networks were constructed by orthogonal pillar[10]arene-based host–guest molecular recognition, terpyridine–Zn^{2+}, and carbene–Ag^+ coordination.

Dalton Transactions Accepted Manuscript

Reversible formation of supramolecular polymer networks *via* orthogonal pillar[10]arene-based host–guest interactions and metal ion coordinations

Lintao Wu[1], Chun Han[1], Xi Wu[1], Lei Wang[2], Yaozi Caochen[2], Xiaobi Jing[2]*

[1]*Department of Chemistry, Changzhi University, Changzhi, Shanxi, 046011 (China).*
[2]*College of Chemistry and Chemical Engineering, Yangzhou University, Yangzhou, Jiangsu, 225002 (China).*

Email address: xbjing@yzu.edu.cn

Electronic Supplementary Information (9 pages)

1. Materials and methods

All reagents were commercially available and used as supplied without further purication. P_{10} was prepared according previous relevant reports.[S1] ^1H or ^{13}C NMR spectra were recorded with a Bruker Avance DMX 500 spectrophotometer or a Bruker Avance DMX 400 spectrophotometer with use of the deuterated solvent as the lock and the residual solvent or TMS as the internal reference. Mass spectra were obtained on a Bruker Esquire 3000 plus mass spectrometer (Bruker-Franzen Analytik GmbH Bremen, Germany) equipped with an ESI interface and an ion trap analyzer. HRMS were obtained on a WATERS GCT Premier mass spectrometer. Viscosity measurements were carried out with a Cannon-Ubbelohde semi-micro dilution viscometer at 25.0 °C in acetonitrile. Scanning electron microscopy investigation was carried out on a JEOL 6390LV instrument. The fluorescence spectra were recorded on a Perkin Elmer LS55 fluorescence spectrophotometer. UV–Vis spectra were taken on a Perkin-Elmer Lambda 35 UV–Vis spectrophotometer.

2. Synthesis of ligand 1
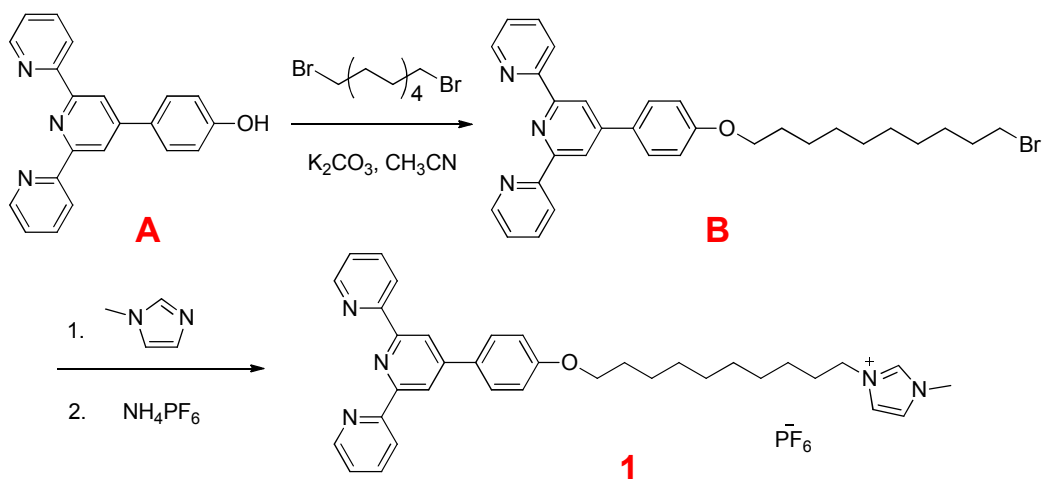
Scheme S1. Synthesis route to ligand **1**.

In a 500 mL round–bottom flask, compound **A** (3.25 g, 10.0 mmol), K_2CO_3 (3.31 g, 24.0 mmol), 1,10-dibromodecane (5.40 g, 18.0 mmol) and acetonitrile (300 mL) were added. The reaction mixture was stirred at reflux for 48 hours. After the solid was filtered off, the solvent was removed. The solid was dissolved in $CHCl_3$ (200 mL) and washed twice with H_2O (200 mL). The organic layer was dried over anhydrous Na_2SO_4 and evaporated to afford the crude product, which was recrystallized with CH_3CN to give the intermediate **B** as a white solid (4.35 g, 80.0 %) as a white solid. The proton NMR spectrum of **B** is shown in Fig. S1. ^{1}H NMR (400 MHz, $CDCl_3$, 298K) δ (ppm): 8.73-8.66 (m, 6H), 7.88-7.86 (t, J = 4 Hz, 4H), 7.36-7.33 (m, 2H), 7.03-7.01 (d, J = 8 Hz, 2H), 4.04-4.01 (d, J = 12 Hz, 2H), 3.43-3.40 (d, J = 12 Hz, 2H), 1.90-1.79 (m, 4H), 1.59-1.33 (m, 12H).

In a 50 mL round–bottom flask, compound **B** (1.09 g, 2.0 mmol), methylimidazole (0.82 g, 10.0 mmol), and toluene (20 mL) were added. The reaction mixture was stirred at reflux for 24 hours. Then the solvent was removed. The solid was dissolved in water (20 mL). Then upon addition of aqueous solution of NH_4PF_6, a white precipitate **1** (1.24g, 90%) was prepared. The proton NMR spectrum of **1** is shown in Fig. S2. ^{1}H NMR (400 MHz, CD_3CN, 298K) δ (ppm): 8.72-8.64 (m, 6H), 8.34 (s, 1H), 7.98-7.89 (m, 2H), 7.84 (s, 2H), 7.45-7.42 (t, J = 4 Hz, 2H), 7.34-7.31 (d, J = 8 Hz, 2H), 7.15-7.12 (t, J = 6 Hz, 2H), 7.06 (s, 1H), 7.04 (s, 2H), 4.09-4.03 (m,

4H), 4.00 (s, 3H), 1.94-1.75 (m, 4H), 1.47-1.43 (m, 2H), 1.31 (s, 12H). The ^{13}C NMR spectrum of **1** is shown in Fig. S3. The ^{13}C NMR (100 MHz, CD3CN, 298K) δ (ppm):160.12, 156.43, 155.83, 149.11, 136.86, 128.50, 123.76, 121.39, 118.26, 114.87, 68.12, 34.06, 32.84, 29.45, 29.37, 29.26, 28.76, 28.18, 26.04. LRESIMS is shown in Fig. S4: m/z 546.7 $[1 - PF_6]^+$. HRESIMS: m/z calcd for $[1 - PF_6]^+$ $C_{35}H_{40}N_5O$, 546.3200; found, 546.3200; error 0 ppm.
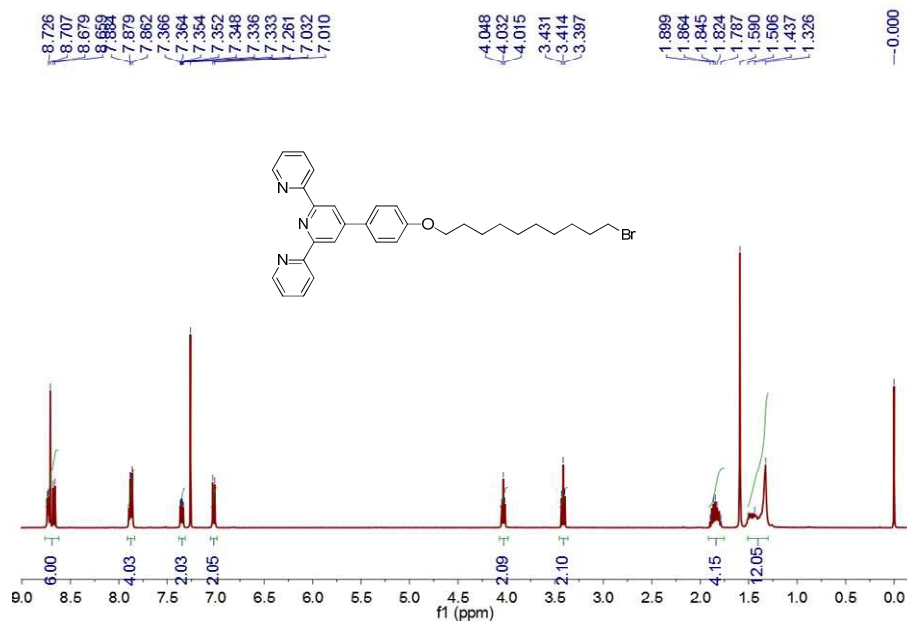
Fig. S1 ^{1}H NMR spectrum (400 MHz, CDCl$_3$, 298K) of **B**.
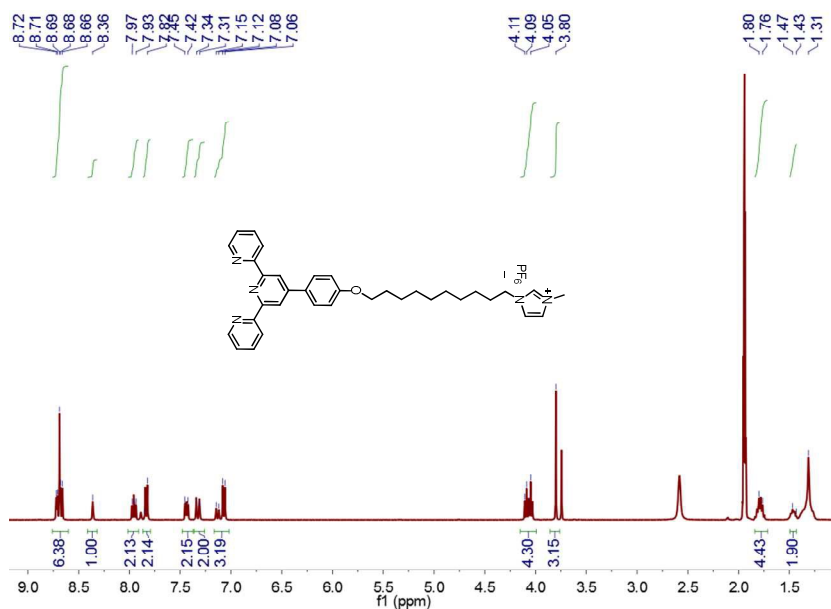
Fig. S2 ^{1}H NMR spectrum (400 MHz, CD$_3$CN, 298K) of ligand **1**.
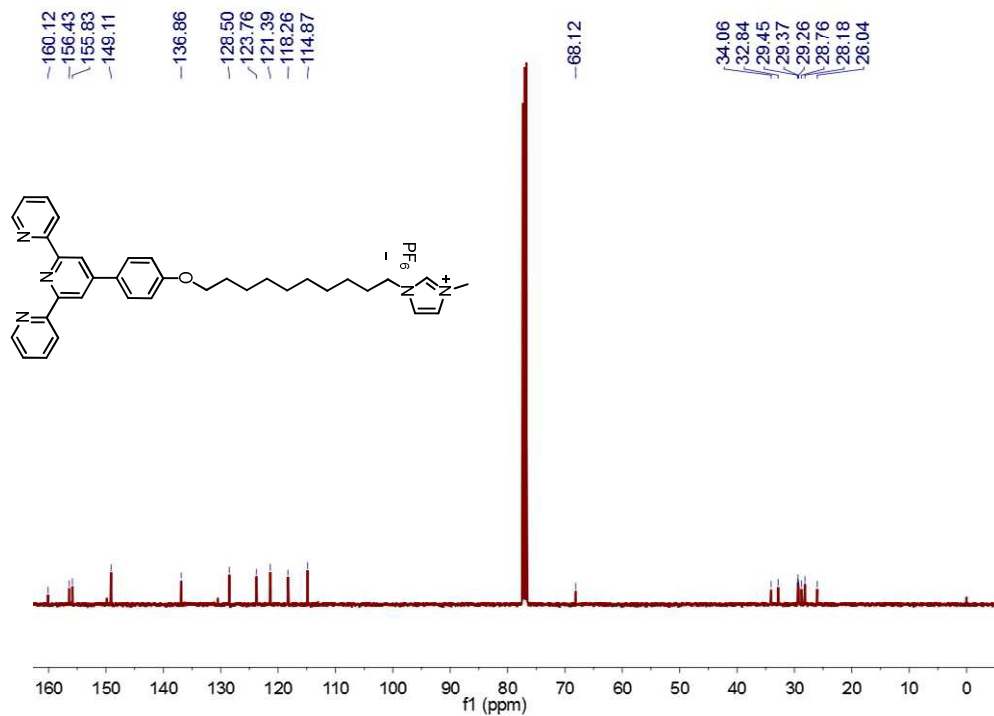
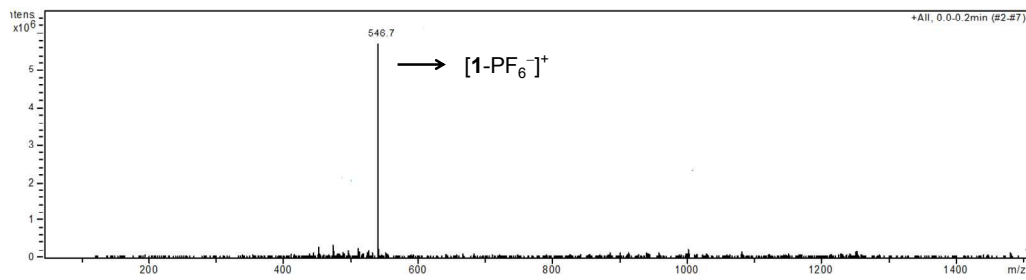**Fig. S3** ^{13}C NMR spectrum (100 MHz, CD$_3$CN, 298K) of ligand **1**.

Fig. S4 Electrospray ionization mass spectrum of ligand **1**. Assignment of the main peak: *m/z* 546.7 [**1** – PF$_6$]$^+$.
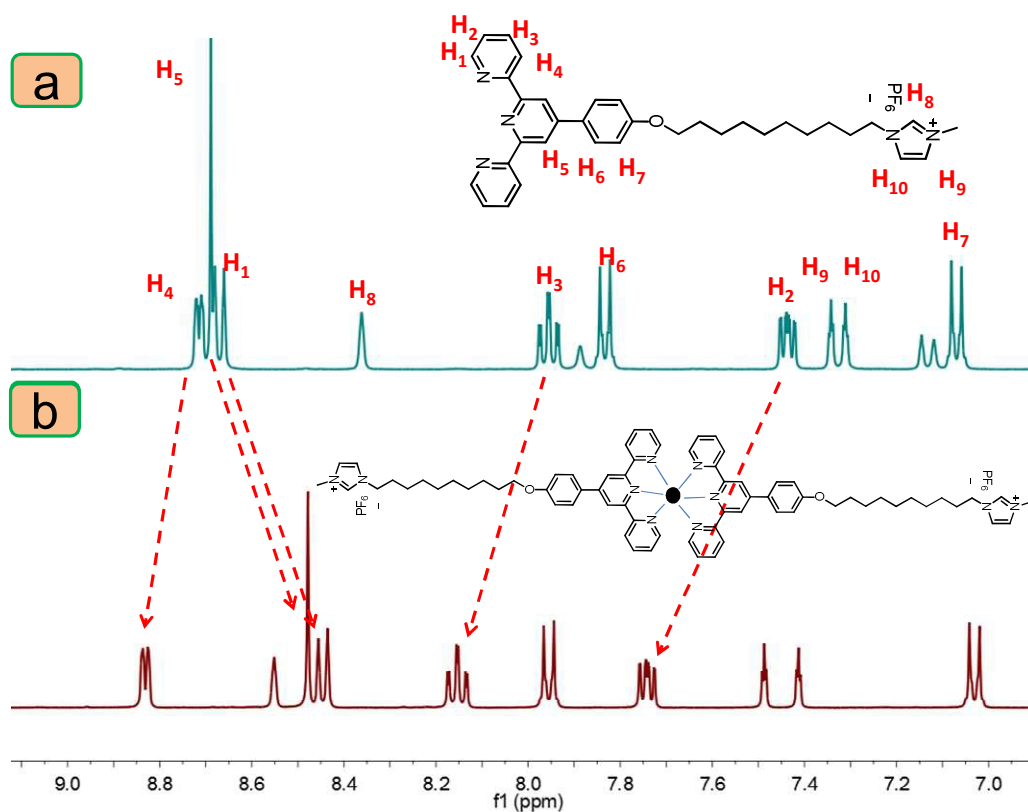
3. Synthesis of dimeric complex 3

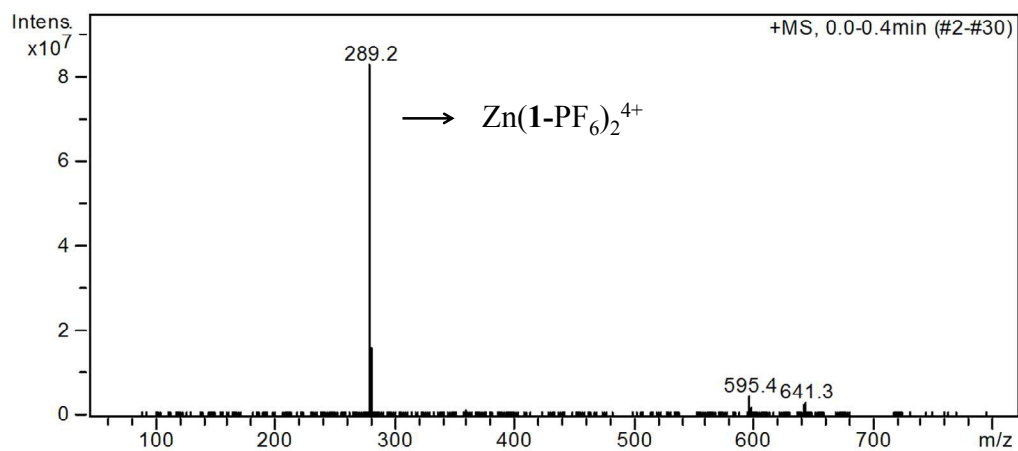**Fig. S5** partial ^{1}H NMR spectrum (400 MHz, CD$_3$CN, 25 °C) of (a) ligand **1** and (b) dimeric complex **3**.

Fig. S6 Electrospray ionization mass spectrum of dimeric complex **3**. Assignment of the main peak: m/z 289.2 [Zn(**1** − PF$_6$)$_2$]$^{4+}$.
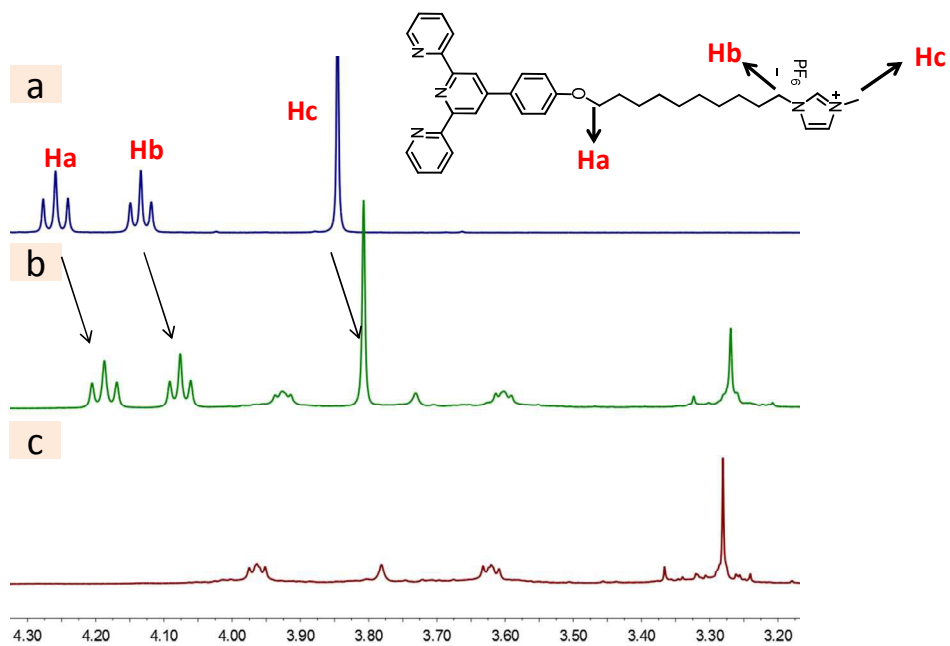
4. Host–guest complexation between 1 and P$_{10}$

Fig. S7 partial ^{1}H NMR spectrum (400 MHz, CD$_3$CN, 25 °C) of (a) ligand **1**, (b) **P$_{10}$** and ligand **1**, (c) **P$_{10}$**.
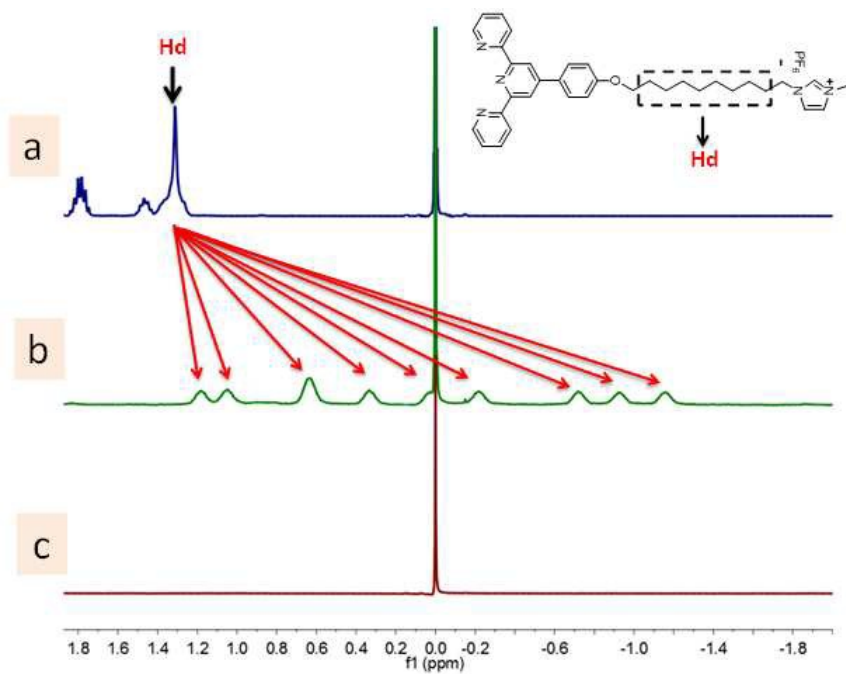
Fig. S8 partial ^{1}H NMR spectrum (400 MHz, CD$_3$CN, 25 °C) of (a) ligand **1**, (b) **P$_{10}$** and ligand **1**, (c) **P$_{10}$**.

5. CF3COOH responsive transformation

As shown in Fig. S9, the signal of imidazolium proton H_8 disappeared, indicating the formation of carbine-Ag complex. More interestingly, the signal of H_8 reappeared by adding CF_3COOH, which is attributed to the stronger binding ability between Ag^+ and CF_3COOH. However, when we added NaOH into the solution of linear supramolecular polymer **A**, the signal of H_8 remained the same, suggesting that the complexation was not simply pH-reponsive.
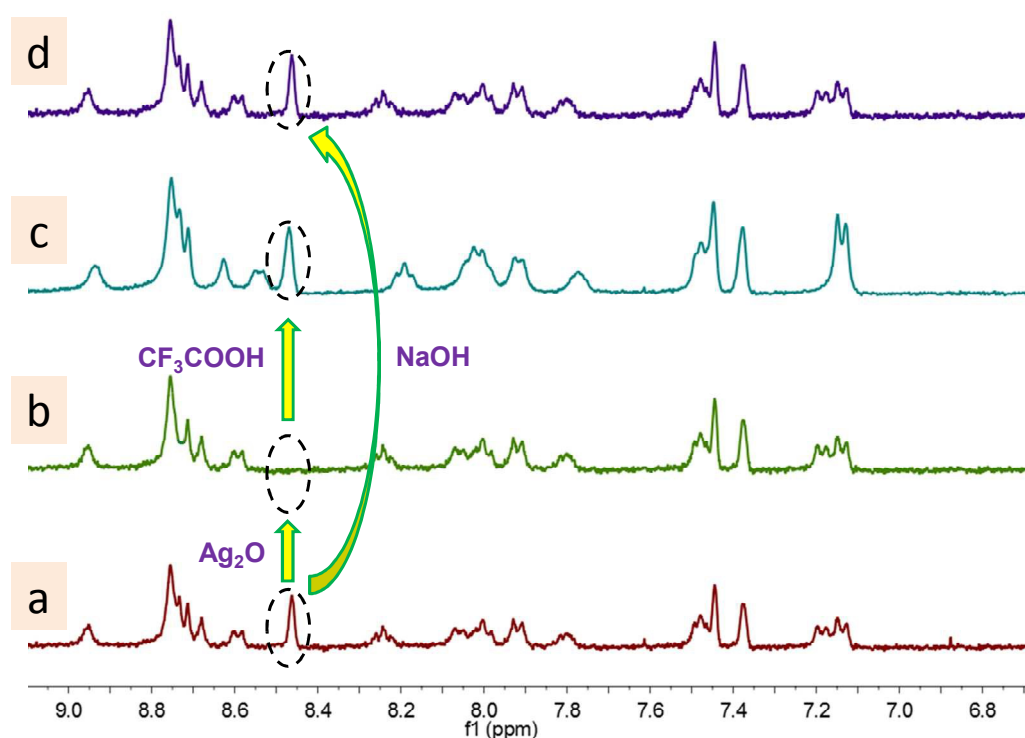

Fig. S9 Partial ^1H NMR spectra (400 MHz, CD_3CN, 25 °C): (a) linear supramolecular polymer **A**; (b) linear supramolecular polymer **A** and excess Ag_2O; (c) after addition of excess CF_3COOH to (b); (d) after addition of excess NaOH to (a).

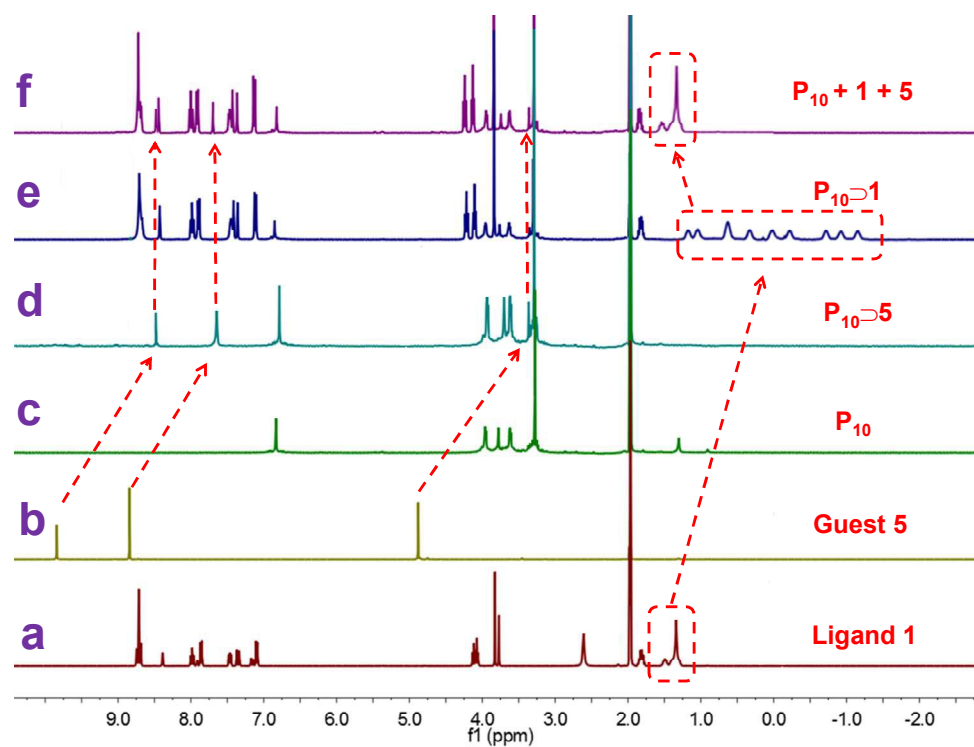### 6. Competitive host-guest interactions between P10 and 1 or 5

Fig. S10 Partial ^{1}H NMR spectra (400 MHz, CD$_3$CN, 25 °C): (a) ligand **1**; (b) guest **5**; (c) **P$_{10}$**; (d) **P$_{10}$⊃5**; (e) **P$_{10}$⊃1**; (f) **P$_{10}$ + 1 + 5**.

7. Refrences

S1. (*a*) T. Ogoshi, T. Aoki, R. Shiga, R. Iizuka, S. Ueda, K. Demachi, D. Yamafuji, H. Kayama, and T.-a. Yamagishi, *J. Am. Chem. Soc.*, 2012, **134**, 20322 −20325; (*b*) X. Chi, and M. Xue, *RSC Adv.*, 2014, **4**, 365–368; (*c*) G. Yu, J. Zhou, and X. Chi, *Macromol. Rapid Commun.*, 2015, **36**, 23−30.